Control of an inverted pendulum using MODE-based Optimized LQR controller

Ismaila B. Tijani
Electronics Eng. Dept., ADMC, HCT, Abu Dhabi, UAE
tijani.ismail@hct.ac.ae

Rini Akmeliawati, Ayodele .I. Abdullateef
Intelligent Mechatronics System Research unit, Faculty of Engineering, IIUM, Malaysia
rakmelia@iium.edu.my.

Abstract— **This paper presents an evolutionary optimization based LQR controller design for an inverted pendulum system. The objective is to address the challenges of appropriate design parameters selection in LQR controller while providing optimal performance compromise between the system control objectives with respect to pendulum angle and position response. Hence, a Multiobjective differential evolution algorithm is proposed to design an LQR controller with optimal compromise between the conflicting control objectives. The performance of the MODE-based LQR is benchmarked with an existing controller from the system manufacturer (QANSER). The performance shows the effectiveness of the proposed design algorithm, and in addition provides an efficient solution to conventional trial and error design approach.**

Keywords—Inverted pendulum system, LQR, Multiobjectives differential evolution,

I. INTRODUCTION *(HEADING 1)*

Inverted pendulum (IVP) system has been one of the major benchmark problems among the control system community. This is attributed to vast practical engineering applications of the IVP system, such as in missiles and rockets, self balancing robots, future transport vehicles like Segway, jetpacks etc. In addition, the complexity of the system dynamics and nonlinear characteristics make it suitable for teaching and practical demonstration of modern control techniques. Several control strategies ranging from model-based control approach such as; classical PID controller, LQR, robust control [1,2] to non-model based approach using artificial intelligent techniques such Fuzzy logic control, Neural network control [3,4], have been reported. Meanwhile, the design of model based controllers is majorly characterized with selection and tuning of one or more design parameters which are usually carried out using trial and error experimentation. For instance, in the LQR controller, the selection and tuning of design Q and R matrices represents major challenges towards achieving satisfactory performance. Considering the complex nonlinear characteristics of IVP system, coupled with conflicting performance objectives to be met with respect to simultaneous balancing of the pendulum and maintaining good cart position response, the tuning of the design parameters using the conventional approach poses non-trivial challenges. Apart from difficulty and time consuming effort require in the design process, the classical design approach does not guarantee an optimal compromise between the control objectives.

These problems have necessitated the use of evolutionary optimization (EOA) techniques for the controller design. Several EOA techniques such as genetic algorithm, (GA), particle swarm optimization (PSO), and differential evolution (DE) have been reported in the LQR controller synthesis [5]. Recently, a Pareto-based Multiobjective Differential Evolution (MODE) algorithm was proposed for model-based controllers' synthesis in [6]. The proposed algorithm has been succesfully used to design full state feedback LQR controller with integral for a 3 degree of freedom (3DOF) helicopter [7]. Briefly, MODE is an extention of Differential Evolution originally proposed by Storn and Price [8] to multobjective optimization problem (MOP). This study presents extention of this previous study by the authors to IVP system. Hence, the control of IVP system is formulated as a constrained MOP which is then solved using the Pareto-based MODE algorithm to obtain an optimized MODE-LQR. The performance of the resulting MODE-LQR is benchmarked with LQR controller provided by the manufacturer of the IVP system used in this study.
Next Section of the paper presents the system description together with mathematical model and control objectives. Overview of LQR control problem formulation is given in Section 3 which is followed by the MODE-Based LQR control design in Section 4. The benchmarking, results and discussion are provided in Section 5. The paper is concluded in Section 6.

II. SYSTEM DESCRIPTION AND CONTROL OBJECTIVES

A rotary inverted pendulum by Quanser [9] is employed in this study. As shown in Figure 1, the system consists of a flat arm (pendulum) mounted to a rotary servo plant (cart), thereby resulting in a horizontal rotating arm with a pendulum at the end. The system is equipped with potentiometer and encoder sensors to measure the pendulum deflection angle, α , and pendulum angular position , θ , respectively.

A. Mathematical Model

The system could be represented as a lump mass at half the lenght of the pendulum as shown in Figure 2. Nonlinear equations of motion of the system are derived based on Euler-Langragian formula. Brief derivation of these equations is repeated here while the detailed derivation of these equations are given in [9].

978-1-4673-6322-8/13/$31.00 ©2013 IEEE

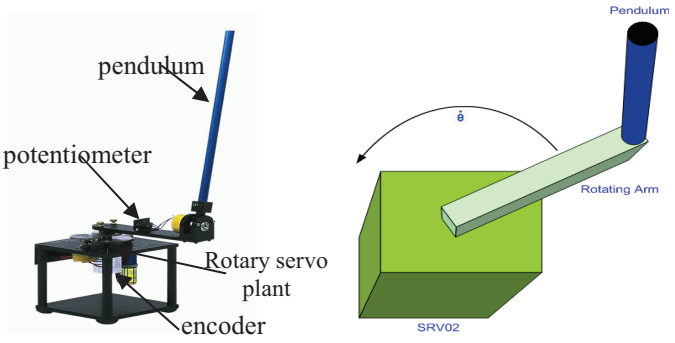

Figure 1: Quanser rotary inverted pendulum system and its top view [9].

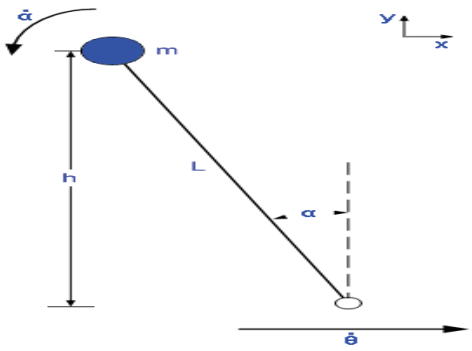

Figure 2: Side view with pendulum in motion [9]

Considering the generalized coordinates (Lagrangian coordinates) θ and α describing the system, the two generalized Euler-Lagragian equations are given by:

$$\frac{\partial}{\partial t}\left(\frac{\partial \Phi}{\partial \dot{\theta}}\right)-\frac{\partial \Phi}{\partial \theta}=T_{output}-B_{eq}\dot{\theta} \tag{1a}$$

$$\frac{\partial}{\partial t}\left(\frac{\partial \Phi}{\partial \dot{\alpha}}\right)-\frac{\partial \Phi}{\partial \alpha}=0 \tag{1b}$$

where Φ is the lagrangin resulting from potential energy, ($E_{P.E.}$) and kinetic energy ($E_{K.E.}$) of the system, T_{output} is the output torque on the load from the motor and B_{eq} is the equivalent friction constant.

The only $E_{P.E.}$ in the system is due to gravity, and is given by:

$$E_{P.E.}=mgh=mgL\cos\alpha \tag{2}$$

The $E_{K.E.}$ in the system arises from the moving hub ($E_{K.E.}^{Hub}$), the velocity of the point mass in the x-direction ($E_{K.E.}^{Vx}$), the velocity of the point mass in the y-direction, ($E_{K.E.}^{Vy}$), and the rotating pendulum about its center mass, ($E_{K.E.}^{pendulum}$). Hence, the total $E_{K.E.}^{Total}$ in the system is expressed as:

$$\begin{aligned}E_{K.E.}^{Total}&=K.E._{Hub}+K.E._{Vx}+K.E._{Vy}+K.E._{pendulum}\\&=\frac{1}{2}J_{eq}^{2}\dot{\theta}^{2}+\frac{1}{2}mV_{x}^{2}+\frac{1}{2}mV_{y}^{2}+\frac{1}{2}J_{cm}^{2}\dot{\alpha}^{2}\end{aligned} \tag{3}$$

where J_{eq} is equivalent inertial of the hub, J_{cm} inertial of the pendulum about its center of mass, V_x and V_y are velocity of the components of the pendulum in x- and y- direction, respectively.

V_x and V_y can be shown to be [10]:

$$V_x=r\dot{\theta}-L\cos\alpha(\dot{\alpha}) \tag{4a}$$

$$V_y=-L\sin\alpha(\dot{\alpha}) \tag{4b}$$

Substituting equations (4a) and (4b), in equation (3), the total kinetic energy becomes:

$$\begin{aligned}E_{K.E.}^{Total}&=\frac{1}{2}J_{eq}^{2}\dot{\theta}^{2}+\frac{1}{2}m\left(r\dot{\theta}-L\cos\alpha(\dot{\alpha})\right)^{2}+\frac{1}{2}m\left(-L\sin\alpha(\dot{\alpha})\right)^{2}\\&\quad+\frac{1}{2}J_{cm}^{2}\dot{\alpha}^{2}\end{aligned} \tag{5}$$

The Lagrangian, Φ, is thus expressed as :

$$\begin{aligned}\Phi=E_{K.E.}^{Total}-E_{P.E.}&=\frac{1}{2}J_{eq}^{2}\dot{\theta}^{2}+\frac{2}{3}mL^{2}\dot{\alpha}^{2}-mLr\cos\alpha(\dot{\alpha})(\dot{\theta}^{2})\\&\quad+\frac{1}{2}mR^{2}\dot{\theta}^{2}-mgL\cos\alpha\end{aligned} \tag{6}$$

By substituting equation (6) in equation (1), the solution of equation (1) yields a linearized equations of motion about $\alpha=0$:

$$\left(J_{eq}+mr^{2}\right)\ddot{\theta}-mLr\ddot{\alpha}=T_{output}-B_{eq}\dot{\theta} \tag{7}$$

$$\frac{4}{3}mL^{2}\ddot{\alpha}-mLr\ddot{\theta}-mgL\alpha=0 \tag{8}$$

The total output torque can be obtained using Kirchhoff's and Newton laws applied to the DC motor of the system as:

$$T_{output}=\frac{\eta_m\eta_g K_t K_g\left(V_m-K_g K_m\dot{\theta}\right)}{R_m} \tag{9}$$

The state space representation of the system is obtained by combining equations (7) to (8)

$$\begin{bmatrix}\dot{\theta}\\ \dot{\alpha}\\ \ddot{\theta}\\ \ddot{\alpha}\end{bmatrix}=\begin{bmatrix}0&0&1&0\\ 0&0&0&1\\ 0&\frac{bd}{E}&\frac{-cG}{E}&0\\ 0&\frac{ad}{E}&\frac{-bG}{E}&0\end{bmatrix}\begin{bmatrix}\theta\\ \alpha\\ \dot{\theta}\\ \dot{\alpha}\end{bmatrix}+\begin{bmatrix}0\\ 0\\ c\frac{\eta_m\eta_g K_t K_g}{R_m E}\\ c\frac{\eta_m\eta_g K_t K_g}{R_m E}\end{bmatrix}u_m \tag{10}$$

where:

$$a=J_{eq}+mr^{2};\ b=mLr;\ c=\frac{4}{3}mL^{2};\ d=mgL;$$

$$E=ac-b^{2};\ \text{and}\ G=\frac{\eta_m\eta_g K_t K_m K_g^{2}+B_{eq}R_m}{R_m}$$

By substituting the values of the system parameters available in [9], the state space model becomes:

$$\begin{bmatrix}\dot{\theta}\\ \dot{\alpha}\\ \ddot{\theta}\\ \ddot{\alpha}\end{bmatrix}=\begin{bmatrix}0 & 0 & 1 & 0\\ 0 & 0 & 0 & 1\\ 0 & 39.32 & -14.52 & 0\\ 0 & 81.78 & -13.98 & 0\end{bmatrix}\begin{bmatrix}\theta\\ \alpha\\ \dot{\theta}\\ \dot{\alpha}\end{bmatrix}+\begin{bmatrix}0\\ 0\\ 25.54\\ 24.59\end{bmatrix}u_m \tag{11}$$

B. Control Objectives

The objective of control system design is to achieve the system stability together with the following specifications [9]:

i. The controller must accurately place the servo angle (θ) at a given command while maintaining the pendulum angle in the upright position

ii. The pendulum angle must not exceed $\pm 6^{\circ}$ when the system is excited with a step input to the θ command.

iii. The control signal, (u_m) must be strictly bounded by ± 2.5 Volts.

iv. The settling time of θ and α should not exceed 2 seconds for a step input.

The challenges of this control problem emanated from the conflicting nature of the duo objectives of maintaining an upright inverted pendulum (minimizing α deflection) and accurate position control of θ. In addition, satisfying the constraints imposed by specifications (ii) to (iv) represent a non-trial performance goal. Achieving these objectives in optimal/sub-optimal sense, calls for a better design strategy over the conventional trial and error control parameters selection.

III. LQR CONTROL FORMULATION OVERVIEW

Given a linear time invariant state-space model of the system as described in section 2, such that:

$$\begin{aligned}\dot{x} &= Ax + Bu\\ y &= Cx + Du\end{aligned} \tag{12}$$

where $x \in \Re^n$ are the states, $u \in \Re^m$ are the inputs and $y \in \Re^p$

For the LQR full-state feedback control approach, the objective is to compute the feedback gains K_{lqr} that minimizes the quadratic cost function given as:

$$\min J = \int_0^{\infty} (\hat{x}^T Q \hat{x} + u^T R u) \tag{13}$$

such that the control signal $u = -K_{lqr} x$

where the matrices Q and R are symmetric positive semidefinite and positive definite weigthing matrices respectively.

The matrices Q and R are the main design parameters to be selected by the designer to satisfy the desired control objectives. In general as indicated in the expression (13), the matrices affects the achievable performance [10]. Therefore, the selection of Q and R parameters greatly influence the success of the LQR controller synthesis. Moreso, with availability of many softwares to solve the required riccati optimal equations involved in the computation of the LQR gains, the major design effort in the controller synthesis has been on the tunning of the weigthing matrices for a given system. The main conventional design procedures are summarized in steps as follows:

Step 1: Specification of matrices Q and R dimension: $Q \in \Re^{n \times n}$, and $R \in \Re^{m \times m}$ diagonal matrices.

Step 2: Selection of parameters of the matrices Q and R diagonal elements, and verify their positive semidefiniteness.

Step 3: Compute the optimal LQR gains K_{lqr} using any of the available software, e.g., for MATLAB users: this can be computed using the command [K,S,E]=lqr(A,B,Q,R).

Step 4: Simulate the resulting close-loop system with the feedback gains obtained in step 3 for a given initial states

Step 5: Evalute the close-loop responses in terms of: state responses, control input, and other desire time-domain specifications.

Step 6: if step 5 results are satisfactory, then proceed to step 7 else, repeat steps 2 to step 5.

Step 8: Choose the controller with best combination of Q and R

Step 9: end

Experience reveals that for a given system, several iterations between step 2 and step 5 are required to obtain satisfactory performances depending on the dimension and complexity of the problem under consideration. In the subsequent sections, the application of MODE is presented to address this challenges leading to an optimized-LQR design approach.

IV. MODE-BASED LQR CONTROLLER DESIGN

Given the state space model representation (11) of the IVP with *n* states and *m* inputs, and the control objectives stated in Section II.C, the goal of the optimization problem is to search for the set of the decision variables, φ, involving the parameters of the weighting matrices Q and R:

$\varphi := [q_1 \ldots q_n, r_1 \ldots r_m]$

that minimizes

the cost function $\min J = \int_0^{\infty} (\hat{x}^T Q \hat{x} + u_m^T R u_m)$ (14)

and set of obejctives of size Ψ: $\min f_i(\varphi)$ $i = 1,2,\ldots \Psi$

subject to: $u_m \le \pm 2.5$; $t_s^{(*)} \le 2$ and $\max\{\alpha\} \le 6^{\circ}$

and $Q \ge 0$ and $R > 0$ with $0 < \varphi_j < H_j$

where H_j is the upper bound on the decision variables, φ.

The objective function $f_i(\varphi)$ is given by the full state feedback system formed by the resulting controller and the IVP system as shown in Figure 3. The objectives are defined by three time domain performances ($\Psi = 3$) for both θ and α:

$$f_i(\varphi) := \left[\max\left\{t_s^{(*)}\right\} \quad \max\left\{O^{(*)}\right\} \quad \max\left\{e_{ss}^{(*)}\right\}\right] \text{ i=1,2,3} \tag{15}$$

where $(*)$ represents θ and α, $t_s^{(*)}$ is the settling time, $O^{(*)}$ is the overshoot, and $e_{ss}^{(*)}$ is the steady state error of the responses.

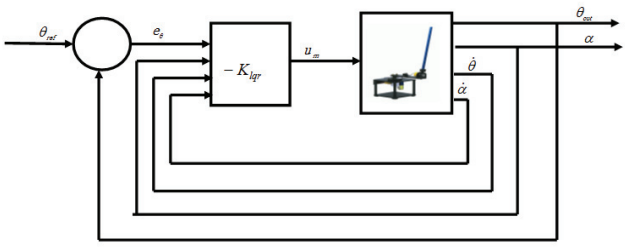

Figure 3: Block diagram of the LQR Full state feedback control system

A. Algorithm Procedure

The Pareto-MODE algorithm proposed in [6] is employed to solve the MOP problem stated in the expression (14). The objective function of the algorithm was modified to solve the feedback system shown in Figure 3, and generate the objective values and constraints for the main MODE algorithm. The main steps involve in the optimization process is summarized here while the detailed of the algorithm can be obtained in [6,7].

Step 1: Specifying the optimization parameters: crossover constant, *CR*, mutation Constant, *F*, population size, NP , decision variable of size, *d*, and maximum generation g_{max}

Step 2: Initialize population, P_o, with feasible individual, of size, NP , for $g = 0$. An individual is feasible if it satisfy the constraints on Q and R matrices and yet yields a stable solution as detailed in [6]. The population comprises of individuals, $\varphi_i^g \ \forall i, i = 1,..., NP$. Given a specified lower, *L*, and upper, *H*, bound on the decision parameters, an individual of the population is initialized using:

$$\varphi_{j,i}^{G=0} = L_i + (H_i - L_i) * rand(1, NP) \quad (16)$$

Step 3: Compute vector of objective values, $f_k(\varphi_i^g)$ for all the individuals in the population

Step 4: Begins MODE optimization process

While g<1 g_{max}

Step 5: Starts DE operation to generate new population, P_{new}

For *i*= 1 to NP

1. Using the DE process of mutation and cross-over, generate new candidate, v_i^{g+1} called child vector from a randomly selected three individuals, r_1, r_2, r_3 , from the previous population such that $r_1, r_2, r_3 \in [1; NP]$, *where* $r_1 \neq r_2 \neq r_3 \neq i$ as follows:

i. Mutation: compute the mutant vector υ using DE operation*:*

$$\upsilon_i = \varphi_{r_3} + F * (\varphi_{r_2} - \varphi_{r_1}) \quad (17)$$

ii. Perform crossover to generate child vector, v_i^{g+1} using:

Generate a random number $Rand_j = floor(rand(0,1) * d)) + 1$

for j=1: d

$$v_{i,j}^{g+1} = \begin{cases} \upsilon_{i,j} & if \ (rand(0,1) \le CR \ \ or \ \ j = Rand_j \\ \varphi_{i,j}^g & otherwise \end{cases} \quad (18)$$

EndFor

2. Check for violation of the bounds *L* and H,

For j=1: d

If $v_{i,j}^{g+1} < L_j \ \backslash\backslash \ v_{i,j}^{g+1} > H_j$

$$v_{i,j}^{g+1} = L_j + (H_j - L_j) * rand(1, NP) \quad (19)$$

EndIf

EndFor

3. Evaluate the objective function of the child vector, $f_k(v_i^{g+1})$.

4. Pareto-selection process: let the generated child vector, v_i^{g+1} compete with the parent vector φ_i^g as follows

$$\varphi_i^{g+1} = \begin{cases} v_i^g : if \ \ v_i^{g+1} \ wins \ \ \varphi_i^g \ \& \ e_d(v_i^{g+1}) \ge \eta, then \ \ i = i+1, \\ \varphi_i^g : if \ \ v_i^{g+1} \ not \ wins \ \ \varphi_i^g \ \& \ e_d(\varphi_i^g) \ge \eta, then \ \ i = i+2, \\ else \ \ i = i, \ repeat \ \ Step \ \ 5 \end{cases} \quad (20)$$

where:

$v_i^{g+1} \ wins \ \ \varphi_i^g \ if \ only \ and \ if :$

$\forall k \in \{1,2,..OB\} : f_k(v_i^g) \le f_k(\varphi_i^g)$

$OR \ \ \exists k \in \{1,2,..OB\} : f_k(v_i^g) < f_k(\varphi_i^g)$

and $e_d(v_i^{g+1})$ and $e_d(\varphi_i^g)$ are the pair wise distance(Euclidean) of the child and parent vectors from the existing solutions in the population, respectively; η is a user specify threshold values that specifies the minimum permissible distance between solutions. For a pair of solutions a and b , e_d is computed as:

$$e_d = \sqrt{(\varphi_1 - \varphi_2)(\varphi_1 - \varphi_2)'} \quad (21)$$

It could be observed from expression (9) that, a trial vector is selected only if, it dominates the current target vector and yet maintains a minimum dissimilarity between the current solutions in the new population. Hence, diversity preservation is incorporated into the Pareto selection.

$P_{new}(i) = \varphi_i^{g+1}$

EndFor

Step 6: Solution archiving: extract non-dominated solutions from P_{new}, and update a secondary population of non-dominated archive. A pre-specified upper bound, γ, on the size of this secondary solution is to be maintained. If the size of this population exceed γ, a crowding distance metric based on computation of Euclidean distance, e_d , (10), between neighboring solutions is employed to remove closed solutions until the size is within the specification.

Step 7: set g=g+1 , and go to Step 4

EndWhileLoop

Step 8: Report the Pareto solutions

B. *Optimization process and results*

The algorithm described in Section IV.B was employed to synthesize LQR controller with the following pre-specified optimization parameters: size of decision variables, $d = 5$; population size, $NP = 30$; generation size, $g_{max} = 200$; crossover constant, $CR = 0.45$, and $\gamma = 30$. The Q matrix parameters is limited to the first two diagonal element in line with the specification used in the reported LQR controller in [10]. This is to give a fair basis for comparative study as reported in Section V. The lower bound on the decision variables, $L = [0 \quad 0 \quad 0]$ and the upper bound, $H = [100 \quad 100 \quad 50]$ based on pre-parameters initialization provided in the MODE algorithm [7].

The final non-dominated Pareto-solutions front is shown in Figure 4. In order to simplify the final selection process, the final Pareto-solutions are reduced to ten candidates (M1 to M10) using the distance metric described in Section 3 to remove closer solutions. Moreover, closer solutions in the pareto-front tend to have little performance differences that may not affect the overall decision. Table 1(a, b) show the parameters and objective values of the resulted ten candidates, while their responses are shown in Figure 5 and Figure 6, respectively for θ and α. As indicated in Table 1, all the candidates satisfy the control objectives stated in Section II.C. Thus any of the controller candidates could be selected based on further preference dictated by the designer or implementation requirement. In this study, a decision matrix (DM) proposed in [6] is used to rate the candidates in order of performance on each objective with least scoring '1' and highest score of '5'. Table 2 shows the DM analysis which provides better insight into the performance compromise. For the sake of further analysis in this study, the candidate with medium total score of _ is selected as a representative candidate known as MODE-LQR.

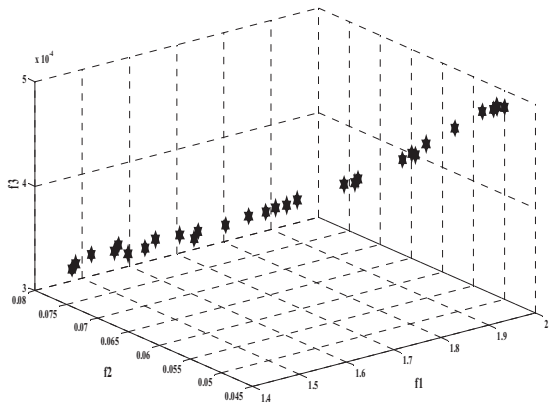

Figure 4: Pareto front of the final non-dominated solutions' objectives

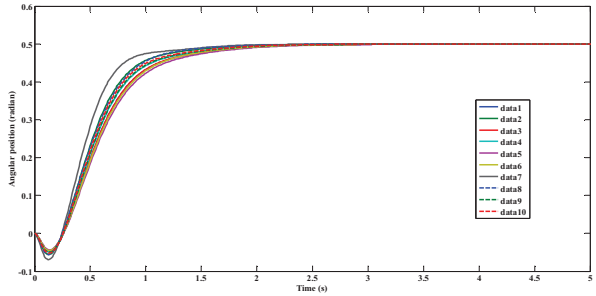

Figure 5: Angular position responses of the five selected solutions

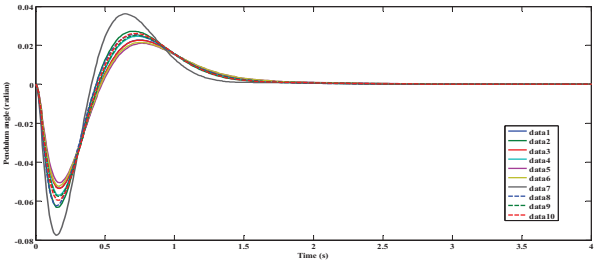

Figure 6: Pendulum angle deflections of the selected five non-dominated solutions

TABLE I. THE TEN PARETO-SOLUTIONS

Candidates	Decision parameters			Objective Values			Constraints		
	Q1	Q2	R	f_1	f_2	f_3	c1	c2	c3
M1	96.306	83.681	22.311	1.75	0.0581	4.16E-04	1.71	1.75	0.058
M2	61.946	94.499	8.564	1.52	0.0687	3.68E-04	2.14	1.52	0.069
M3	78.772	79.245	27.616	2.00	0.0498	4.85E-04	1.42	2.00	0.050
M4	61.946	59.999	19.175	1.92	0.0522	4.62E-04	1.51	1.92	0.052
M5	85.695	10.232	19.463	1.72	0.0590	4.18E-04	1.74	1.72	0.059
M6	41.841	35.842	12.847	1.92	0.0524	4.67E-04	1.51	1.92	0.052
M7	25.040	59.503	5.209	1.72	0.0593	4.07E-04	1.78	1.72	0.059
M8	80.670	33.206	21.717	1.83	0.0553	4.40E-04	1.61	1.83	0.055
M9	30.398	91.092	7.983	1.85	0.0543	4.42E-04	1.60	1.85	0.054
M10	14.368	75.504	3.695	1.87	0.0535	4.35E-04	1.60	1.87	0.054

TABLE II. DECISION MATRIX

Candidates	Score per Objective Values			Total Score
	f_1	f_2	f_3	
M1	8	4	8	20
M2	10	1	10	21
M3	3	10	1	14
M4	4	9	3	16
M5	9	2	7	18
M6	4	8	2	14
M7	9	3	9	21
M8	7	5	5	17
M9	6	6	4	16
M10	5	7	6	18

V. BENCHMARKING

The performance of the MODE-LQR is benchmarked with LQR supplied by the manufacturer of the plant. Figure 7, Figure 8 and Figure 9 show the comparison of the MODE-LQR and Quanser-LQR responses, respectively for θ, α and

the control effort. The numerical overview of performance comparison is presented in Table 3 together with percentage improvement achieved with the proposed MODE-based LQR controller compared to the Quanser-LQR.

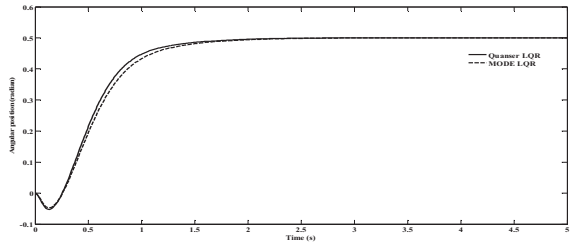

Figure 7: Angular position responses with MODE-LQR and Quanser-LQR

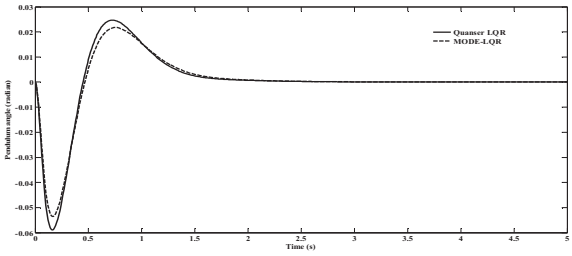

Figure 8: Pendulum angle deflection with MODE-LQR and Qaunser-LQR

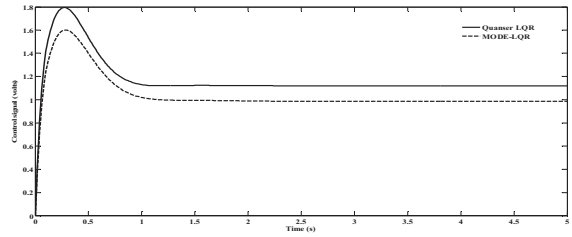

Figure 9: Control signal with MODE-LQR and Qaunser-LQR

As shown in Figure 7 to Figure 9, except in the settling time performance, the proposed MODE-LQR generally gave better performance response over the Quanser-LQR especially in terms of maximum peak response in the pendulum angle and lesser control effort. It should be recalled that, the settling time is part of constraint which has been met by both controllers. Thus, the settling time may not be considered in the overall comparative study. Hence, as shown in Table III, the proposed MODE-based controller gave 9.2% and 11% improvement, respectively in the pendulum swing angle and the control effort. Apart from this response performance, computationally, the proposed optimization algorithm takes approximately 150 seconds (2.5 minutes) to synthesis the controller. Comparing this with conventional design approach which may takes several hours depending on the designer experience and a priori information about the system dynamics, this represents a significant reduction in the design effort and simplified the overall system development especially for a practical applications.

TABLE III. PERFORMANCE COMPARISON

	Thetha			
Models	t_s	O	e_{ss}	$max\ \{\|\mu\|\}$
MODE-LQR	1.790	0.00	0.0004	1.60
Quanser-LQR	1.633	0.00	0.0004	1.80
% improvement	-9.8	0	0	11
	Alpha			
Models	t_s	O	e_{ss}	
MODE-LQR	1.833	0.0535	0.0001	
Quanser-LQR	1.740	0.0589	0.0001	
% improvement	-2.85	9.2	0	

VI. CONCLUSION

A synthesis of Pareto-optimal LQR controller has been presented in this paper for control of an inverted pendulum system using a MODE-based evolutionary algorithm. The results and comparative study have shown the effectiveness this proposed design approach in overcoming the challenges of trail and error tuning of the controller parameters, and yet satisfying conflicting design objectives. This is expected to provide a simplify design approach to IVP-based engineering system in both robotics and space systems applications.

REFERENCES

[1] A.N.K. Nasir, M.A. Ahmad and M.F. Rahmat. Performance Comparison Between LQR And PID Controller for an Inverted Pendulum System. International Conference on Power Control and Optimization, Chiang May, Thailand, 18-20, July 2008

[2] Petr Chalupa and Vladimír Bobál. Modelling and Predictive Control of Inverted Pendulum Proceedings 22nd European Conference on Modelling and Simulation ©ECMS Loucas S. Louca, Yiorgos

[3] Jin Seok Noh, Geun Hyung Lee, and Seul Jung . Position Control of a Mobile Inverted Pendulum System using Radial Basis Function Network. International Journal of Control, Automation, and Systems (2010) 8(1):157-162.

[4] Chen Wei Ji, Fang Lei and Lei Kam Kin. Fuzzy Logic control for an inverted pendulum. IEEE Conference on Intelligent systems, 1997.

[5] S. Amir Ghoreishi, Mohammad Ali Neloni and S. Omid Basiri (2011). Optimal Design of LQR Weigthing Matrices based on Intelligent Optimization Methods, International Journal of Intelligent Inofrmation Processing, vol. 2,no 1, March,2011.

[6] Tijani I.B.. Flight control system with MODE based H-infinity for small scale autonomous helicopter. PhD thesis submitted to Mechatronics engineering department, IIUM,Malaysia, October 2012.

[7] Tijani I.B, Rini Akmeliawati, Ari Legowo, and A. G. Abdul Muthalif, 2011. "Optimization of PID controller for Flexible link system using a Pareto-based Multi-Objective differential (PMODE) evolution", accepted for publication in the 4th International Conference on Mechatronics, 2011 (ICOM'11), KL, Malaysia.

[8] Storn, R. and Price, K., 1997. Differential Evolution – A Simple and Efficient Heuristic for Global Optimization over Continuous Spaces, Journal of Global Optimization 11: 341–359, 1997, 341 1997 Kluwer Academic Publishers.

[9] The Quanser Consulting Inc. User manual for Rotary pendulum, Revision 01, 2006.

[10] Brian L. Stevens and Frank L. Lewis. Aircraft control and simulation, John Wiley & Sons,1992.